Resuscitation 84 (2013) 1625–1632

Contents lists available at ScienceDirect

Resuscitation

journal homepage: www.elsevier.com/locate/resuscitation

Experimental paper

Detection of a spontaneous pulse in photoplethysmograms during automated cardiopulmonary resuscitation in a porcine model☆,☆☆

Ralph W.C.G.R. Wijshoff[a,*], Toeno van der Sar[b], Wouter H. Peeters[b], Rick Bezemer[b], Paul Aelen[b], Igor W.F. Paulussen[b,c], Simone C.M.A. Ordelman[b], Alyssa Venema[d], Paul F.J. van Berkom[e], Ronald M. Aarts[a,b], Pierre H. Woerlee[b], Gert-Jan Scheffer[f], Gerrit J. Noordergraaf[c]

[a] Signal Processing Systems, Department of Electrical Engineering, Eindhoven University of Technology, Den Dolech 2, 5612 AZ Eindhoven, The Netherlands
[b] Philips Research, High Tech Campus 34, 5656 AE Eindhoven, The Netherlands
[c] Department of Anaesthesiology & Resuscitation and CPRLab, St. Elisabeth Hospital, Hilvarenbeekseweg 60, 5022 GC Tilburg, The Netherlands
[d] Department of Surgery and CPRLab, St. Elisabeth Hospital, Hilvarenbeekseweg 60, 5022 GC Tilburg, The Netherlands
[e] Department of Intensive Care and CPRLab, St. Elisabeth Hospital, Hilvarenbeekseweg 60, 5022 GC Tilburg, The Netherlands
[f] Department of Anesthesiology, Pain and Palliative Medicine, Radboud University Nijmegen Medical Center, Geert Grooteplein 10, 6525 GA Nijmegen, The Netherlands

ARTICLE INFO

Article history:
Received 22 May 2013
Received in revised form 10 July 2013
Accepted 23 July 2013

Keywords:
Cardiopulmonary resuscitation
Chest compressions
Photoplethysmography
Pulse detection
Return of spontaneous circulation

ABSTRACT

Introduction: Reliable, non-invasive detection of return of spontaneous circulation (ROSC) with minimal interruptions to chest compressions would be valuable for high-quality cardiopulmonary resuscitation (CPR). We investigated the potential of photoplethysmography (PPG) to detect the presence of a spontaneous pulse during automated CPR in an animal study.
Methods: Twelve anesthetized pigs were instrumented to monitor circulatory and respiratory parameters. Here we present the simultaneously recorded PPG and arterial blood pressure (ABP) signals. Ventricular fibrillation was induced, followed by 20 min of automated CPR and subsequent defibrillation. After defibrillation, pediatric-guidelines-style life support was given in cycles of 2 min. PPG and ABP waveforms were recorded during all stages of the protocol. Raw PPG waveforms were acquired with a custom-built photoplethysmograph controlling a commercial reflectance pulse oximetry probe attached to the nose. ABP was measured in the aorta.
Results: In nine animals ROSC was achieved. Throughout the protocol, PPG and ABP frequency content showed strong resemblance. We demonstrate that (1) the PPG waveform allows for the detection of a spontaneous pulse during ventilation pauses, and that (2) frequency analysis of the PPG waveform allows for the detection of a spontaneous pulse and the determination of the pulse rate, even during ongoing chest compressions, if the pulse and compression rates are sufficiently distinct.
Conclusions: These results demonstrate the potential of PPG as a non-invasive means to detect pulse presence or absence, as well as pulse rate during CPR.

1. Introduction

High-quality cardiopulmonary resuscitation (CPR) requires minimizing interruptions to chest compressions.[1,2] Pulse checks, even during potentially perfusing rhythms, may lead to prolonged interruptions which can negatively impact outcome.[3–5] In particular, manual palpation can be time-consuming and is known to be unreliable even if performed by expert clinicians.[6–9] Therefore, a rapid, objective method to detect the return of spontaneous circulation (ROSC) would be a valuable asset.

Monitoring of end-tidal CO_2,[10–13] invasive blood pressure,[14,15] or central venous oxygen saturation[16] allows for a more objective assessment of ROSC, but requires a secured airway or placement of catheters. Trans-thoracic impedance (TTI) measurements[17–19] and near-infrared spectroscopy (NIRS)[20–24] are non-invasive, but TTI is strongly influenced by chest compressions[17–19] and NIRS responds slowly upon ROSC.[20,23,24] Despite the challenges, and even though

☆ A Spanish translated version of the summary of this article appears as Appendix in the final online version at http://dx.doi.org/10.1016/j.resuscitation.2013.07.019.
☆☆ Protocol number of the Animal Ethical Committee of the Radboud University Nijmegen Medical Center: RU-DEC 2011-188.

* Corresponding author.
E-mail addresses: ralph.wijshoff@philips.com, r.w.c.g.r.wijshoff@tue.nl (R.W.C.G.R. Wijshoff).

0300-9572/$ – see front matter © 2013 Elsevier Ireland Ltd. All rights reserved.
http://dx.doi.org/10.1016/j.resuscitation.2013.07.019

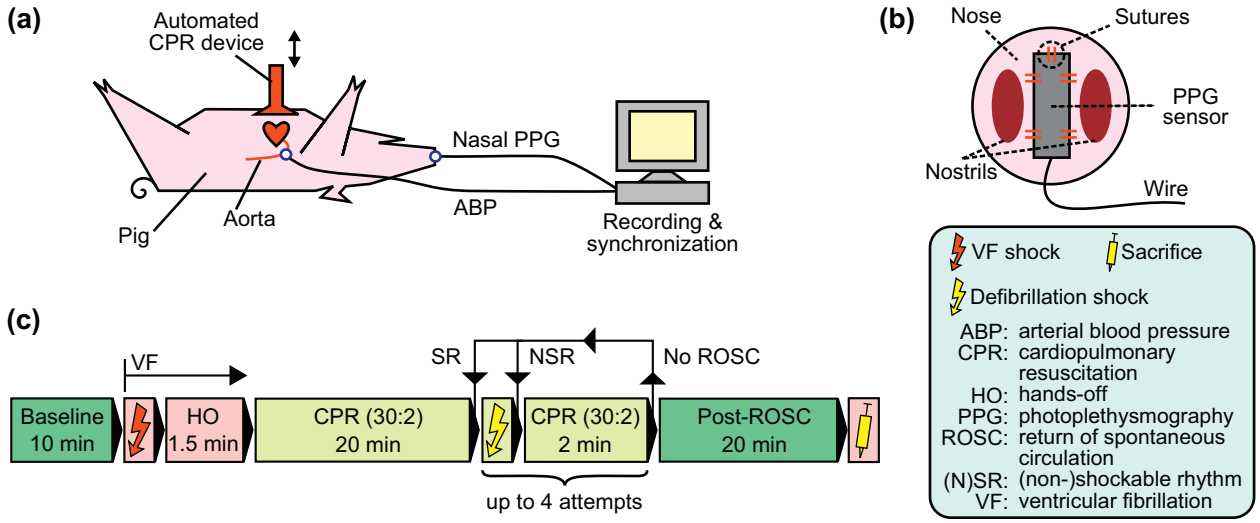

Fig. 1. Simultaneous acquisition of PPG and ABP waveforms during automated CPR in a pig model. (a) Experimental setting. PPG signals have been acquired from the nose. ABP has been measured in the thoracic aorta using a Millar catheter. (b) Attachment of the PPG sensor to the nose. (c) Summary of the experimental protocol. See text for further details.

determining whether an observed rhythm is life-supporting remains a clinical, situational assessment, such techniques can provide valuable support.

CPR guidelines mention the potential of photoplethysmography (PPG) to support ROSC detection.[2] A PPG sensor, such as the well-known finger clip commonly used to monitor arterial oxygen saturation, measures transmission of light through tissue to detect cardiac-induced pulses in tissue blood volume.[25] PPG is generally an easy-to-use and non-invasive technique to measure spontaneous pulse and other hemodynamic parameters,[25–28] but using PPG to detect spontaneous pulse during CPR is not common clinical practice.[29] Interpretation of the PPG signal can be compromised by low perfusion, temperature effects, delays by signal processing, and motion artifacts.[2,30,31] It may also be difficult to determine if pulses in the PPG signal should be attributed to chest compressions or to spontaneous cardiac activity.[30]

In this study, we investigated the potential of PPG to detect the presence and rate of a spontaneous pulse during CPR. We retrospectively analyzed PPG and arterial blood pressure (ABP) signals, simultaneously recorded in pigs undergoing automated CPR. PPG-based detection of a spontaneous pulse during CPR is a first step toward determining the potential use of PPG to support ROSC detection.

2. Methods

2.1. Study design

An automated-CPR animal study was conducted on 16 pathogen-free female Yorkshire pigs, with an average age of 10.7 weeks (range 7–12 weeks) and an average weight of 30 kg (range 25–36 kg) (Fig. 1a). All animals received care in compliance with the Dutch Animal Experimentation Law and the Standard Operation Procedures of the Central Animal Laboratory of the Radboud University Nijmegen Medical Center, where the experiments were conducted. The Radboud University Animal Ethical Committee approved the protocol. The experiments were designed and executed using the Utstein-style guidelines.[32] PPG-based detection of a spontaneous pulse during CPR was a secondary objective of the animal experiments, which were designed to study characteristics of automated-CPR and their relationship to ROSC. Only data pertinent to the PPG study are reported here.

2.2. Anesthesia and management

Animals received intramuscular (IM) premedication with ketamine (10 mg/kg), midazolam (1 mg/kg), and atropine (50 μg/kg). After intravenous (IV) access was gained, propofol (2–3 mg/kg) was administered, and the animals were orally intubated and moved to the operating table. Anesthesia was maintained with isoflurane (0.5–1% end-tidal) via a SmartVent 7900 Anesthesia Ventilator (Datex-Ohmeda, Finland), and by IV infusions of midazolam (0.6 mg/kg/h), sufentanyl (5 μg/kg and 10 μg/kg/h), and vecuronium (0.2 mg/kg and 0.4 mg/kg/h). Amoxicilline (20 mg/kg) was administered IV.

Animals were ventilated through a bacteria-virus filter using an FiO_2 of 0.4 and 6–7 cmH_2O PEEP, with tidal volumes of 275–300 ml at a rate of about 20 min^{-1} to achieve end-tidal CO_2 partial pressures of 30–40 mmHg. Five minutes before induction of cardiac arrest, FiO_2 was increased to 1.0. Following cardiac arrest, ventilation was continued manually with an FiO_2 of 1.0 via a pediatric 500 ml self-inflating bag, without isoflurane, and sufentanyl infusion was stopped.

During instrumentation, warm normal saline (0.9% NaCl) was administered to maintain a mean right-atrial pressure of 6–10 mmHg. Blood loss was compensated for by IV boli of Voluven. Temperature was controlled with a water-filled mattress. Euthanasia was performed with 500 mg pentobarbital (IV bolus).

2.3. Instrumentation and monitoring

Instrumentation and monitoring was performed once the animal was installed on the operating table. End-tidal CO_2 partial pressure, and airway pressure, flow and volume were monitored using spirometry (IntelliVue MP50 Patient Monitor, Philips, Andover, MA, USA). Via cutdown, a 20 G 16 cm cannula was placed in the left ileo-femoral artery for sampling purposes. Mikro-Tip® Pressure Catheters (Model SPC-360S, Millar Instruments, Houston, TX, USA) connected to a PCU-2000 Pressure Control Unit (Millar Instruments, Houston, TX, USA) were placed via the right femoral artery and vein, such that their tips lay just distal to the aortic arch (to measure arterial blood pressure, ABP) and in the inferior vena cava just proximal to the right atrium (to measure central venous pressure), respectively. Via cutdown to the right internal jugular vein, a Swan-Ganz catheter (Edwards Lifesciences, Irvine, CA,

Table 1
Physiological variables of the 12 animals included in the study. Pulse rate, arterial blood pressure, and end-tidal CO_2 were determined during the last 30 s of baseline, 20 min CPR, and 20 min post-ROSC.

	Baseline (12 animals)			20 min CPR (12 animals)			20 min post-ROSC (9 animals)		
	Mean (SD)	Min	Max	Mean (SD)	Min	Max	Mean (SD)	Min	Max
Pulse rate [BPM]	93 (17)	64	124	–	–	–	113 (19)	86	155
Arterial blood pressure [mmHg]									
Mean	107 (10)	97	132	33 (7)	24	46	93 (23)	64	124
Systolic	122 (14)	109	157	59 (16)	36	89	102 (25)	69	135
Diastolic	94 (10)	80	114	18 (6)	10	31	84 (21)	58	114
Arterial blood									
PaO_2 [kPa]	60 (17)	27	77	22 (17)	8	54	48 (17)	19	70
$PaCO_2$ [kPa]	6 (0.3)	5	6	8 (2)	5	11	7 (0.5)	6	7
pH	7.50 (0.04)	7.44	7.60	7.22 (0.09)	7.12	7.39	7.34 (0.06)	7.22	7.41
Lactate [mmol/L]	0.8 (0.4)	0.4	1.8	5 (2)	3	8	4 (1)	3	5
Hb [mmol/L]	4 (0.6)	3	5	–	–	–	5 (0.7)	4	6
SaO_2 [%]	100 (0)	100	100	94 (6)	83	100	100 (0)	99	100
Venous blood									
PvO_2 [kPa]	11 (6)	5	29	3 (0.4)	3	4	7 (2)	6	12
$PvCO_2$ [kPa]	6 (0.8)	4	7	10 (1)	8	12	8 (0.8)	6	9
pH	7.44 (0.03)	7.38	7.50	7.19 (0.05)	7.10	7.29	7.26 (0.05)	7.17	7.32
Lactate [mmol/L]	0.8 (0.4)	0.4	2	4 (1)	3	6	4 (1)	3	6
SvO_2 [%]	91 (8)	72	100	30 (7)	18	39	73 (26)	8	96
End-tidal CO_2 [mmHg]	38 (2)	35	43	39 (8)	27	48	41 (3)	36	45

BPM: beats per minute; CPR: cardiopulmonary resuscitation; Max: maximum; Min: minimum; ROSC: return of spontaneous circulation; SD: standard deviation. Arterial blood pressure was measured with a Millar catheter in the thoracic aorta. Units are indicated in square brackets.

USA) was positioned in the pulmonary artery such that wedge was achieved. A flow sensor (Transonic® Animal Research Flowmeter T206, Transonic Systems Inc., Ithaca, NY, USA) was placed around the right common carotid artery. Catheter positions were confirmed by visual inspection at autopsy.

Raw red (660 nm) and near-infrared (900 nm) PPG signals were obtained using a forehead reflectance pulse oximetry probe (Nellcor™ Oxisensor II RS-10, Covidien-Nellcor™, Dublin, Ireland), controlled by a custom-built photoplethysmograph. The probe was customized to enable placement by suturing between the nostrils (Fig. 1b), because it is a relatively stable measurement site in terms of motion, and it allows tight fixation of the probe to the skin.

PPG and ABP waveforms were recorded simultaneously using a 16 bit digital data acquisition card (DAQ) (NI USB-6259, National Instruments, Austin, TX, USA). A LabVIEW® (National Instruments, Austin, TX, USA) program controlled the DAQ.

2.4. Experimental protocol

The experimental protocol is outlined in Fig. 1c. After instrumentation, a 10 min baseline period, including blood gas analysis, documented the physiological condition of the animal. Subsequently, cardiac arrest was induced with a trans-thoracic electrical shock (90 V, 50 Hz for 3 s, using a proprietary fibrillation device), followed by a 90 s hands-off period. CPR was then performed for 20 min, using a rhythm of thirty compressions and two ventilations (30:2 ratio). Chest compressions were delivered by a LUCAS™2 Chest Compression System[33] (Physio-Control Inc./Jolife AB, Lund, Sweden) or by a custom-built automated CPR device, which was randomly assigned. The compression rate was 100 min^{-1}, and the ventilation pause lasted 3.8 s. No vasoactive medication was given during this period. After 20 min of CPR, rhythm analysis was performed and defibrillation attempted at 4 J kg^{-1} if appropriate, using the HeartStart MRx Monitor/Defibrillator (Philips, Andover, MA, USA) with Adult Plus Multifunction Electrode Pads M3713A (Philips, Andover, MA, USA). CPR was then immediately reinstituted for 2 min, after which the next rhythm analysis and pulse check were performed. If ROSC was diagnosed, CPR was stopped. If ROSC was not achieved, up to three additional 2-min cycles were performed. Starting after the first rhythm analysis, pediatric advanced life-support guidelines were used for medication, volume management, and critical care interventions.[34] Infusion of sufentanyl was also restarted. Measurements were continued up to 20 min post-ROSC. After that, or if ROSC was not achieved after four 2-min cycles, the experiment was ended, the animal was euthanized, and an autopsy was performed.

Blood gases were analyzed from samples drawn simultaneously from the left femoral artery and the right atrium. Blood samples were drawn after 5 min of baseline, at the beginning and end of CPR, 2 min after a second and fourth defibrillation attempt, and at the beginning and end of the post-ROSC period. Samples were analyzed on-site via two i-STAT® Blood Gas Analyzers (Abbott Point of Care Inc., Princeton, NJ, USA).

2.5. Data analysis

The PPG signal, reported in volts, is proportional to the detected light intensity, i.e., an increase in blood volume in the sampled tissue results in a decrease in the PPG signal. The PPG signal was limited in frequency to 11 Hz to reduce the influence of noise. Only the near-infrared PPG signal has been analyzed, because it had a better signal-to-noise ratio than the red PPG signal.[35]

Both PPG and ABP signals were analyzed retrospectively with special interest in the period before and after ROSC. The PPG time traces were analyzed to detect the presence of a spontaneous cardiac pulse. The observations were validated by comparing the PPG signal to the ABP signal. Furthermore, to gain more insight into the origin of the signals, spectrograms were plotted, which show which frequencies are present in the signals as a function of time. These spectrograms were obtained via Fourier transformation of consecutive segments of the time traces.

3. Results

We used PPG and ABP data from 12 out of 16 animals. PPG signals from the first four animals were excluded because of interference between the study probe and the clinical saturation probes. This was resolved by increasing the distance between the probes. Table 1 presents baseline and CPR data of the 12 animals included in our analysis, and the post-ROSC data of the nine animals with ROSC in this group.

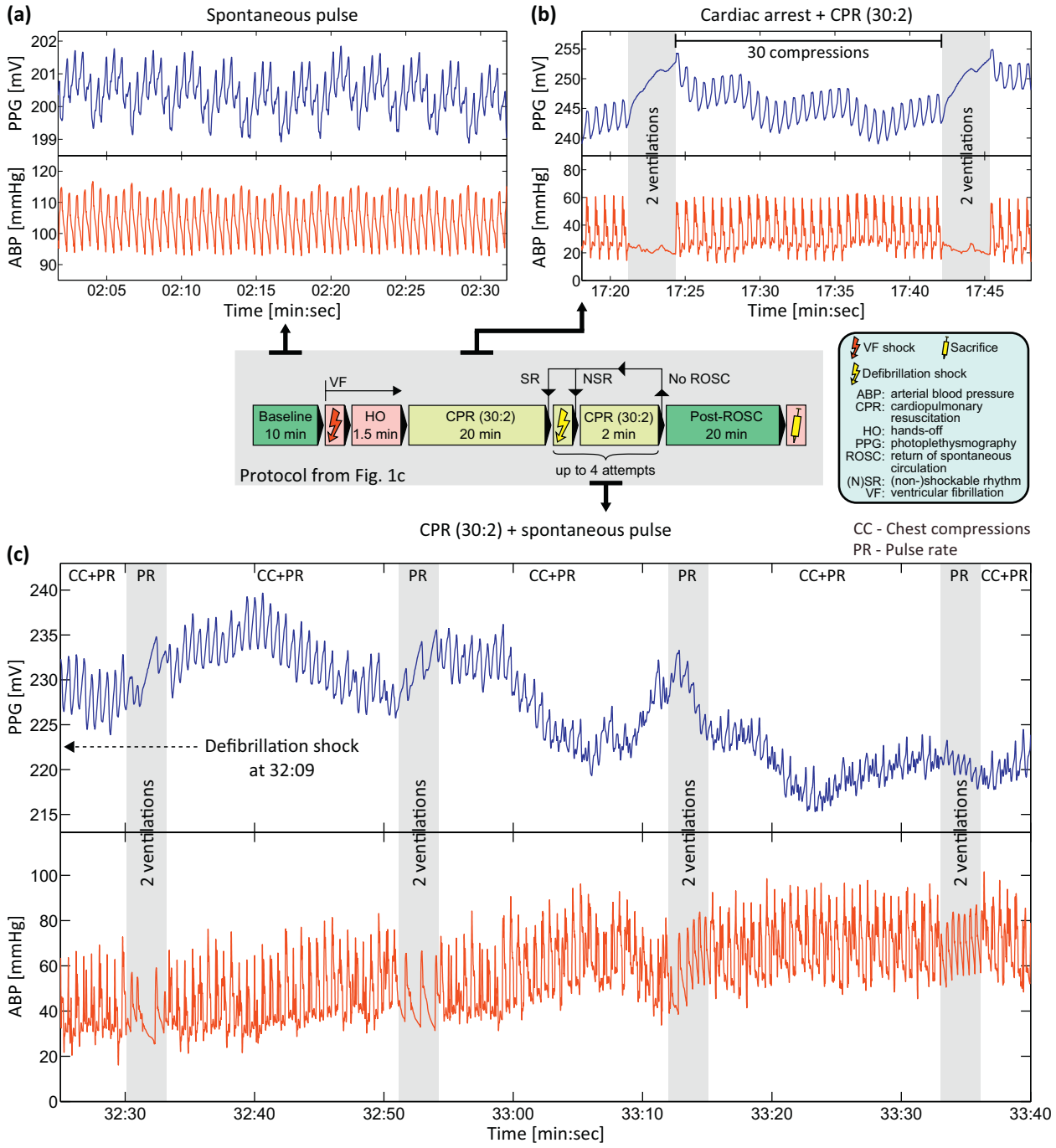

Fig. 2. Distinct morphologies of the PPG and ABP waveforms during different stages of the experiment. (a) Baseline. PPG and ABP waveforms show a spontaneous pulse rate of approximately 110 beats per minute. Continuous ventilation causes slow variations in both PPG and ABP waveforms. (b) CPR during cardiac arrest (ventricular fibrillation). (c) CPR after defibrillation. Traces start 16 s after the shock. As early as the first ventilation pause following successful defibrillation, spontaneous cardiac output can be seen in both PPG and ABP waveforms. This is the same animal (#R1) as in Figs. 3 and 4d.

3.1. Spontaneous pulse during ventilation pauses

Fig. 2 illustrates the different morphologies of the PPG and ABP signals during the CPR protocol. During baseline, cardiac pulses were visible in the PPG and ABP waveforms (Fig. 2a). After induction of cardiac arrest, automated chest compressions caused oscillations in PPG and ABP signals (Fig. 2b), and no spontaneous pulsations could be observed consistent with persisting cardiac arrest. Following successful defibrillation, subsequent ventilation pauses showed pulses at an increasing rate (Fig. 2c).

3.2. Spontaneous pulse during chest compressions

After successful defibrillation, increasing irregularity could be observed in the PPG waveform resulting from the influence of both chest compressions and spontaneous cardiac output (Fig. 2c). Spectrograms of the PPG and ABP signals show the chest compressions at a rate of 100 min^{-1} before and after defibrillation (Fig. 3). In addition, after defibrillation, a disorganized spectral activity appeared, filling the frequency band from 0 to 200 min^{-1}. About 1 min after the shock, a distinct spectral component appeared at

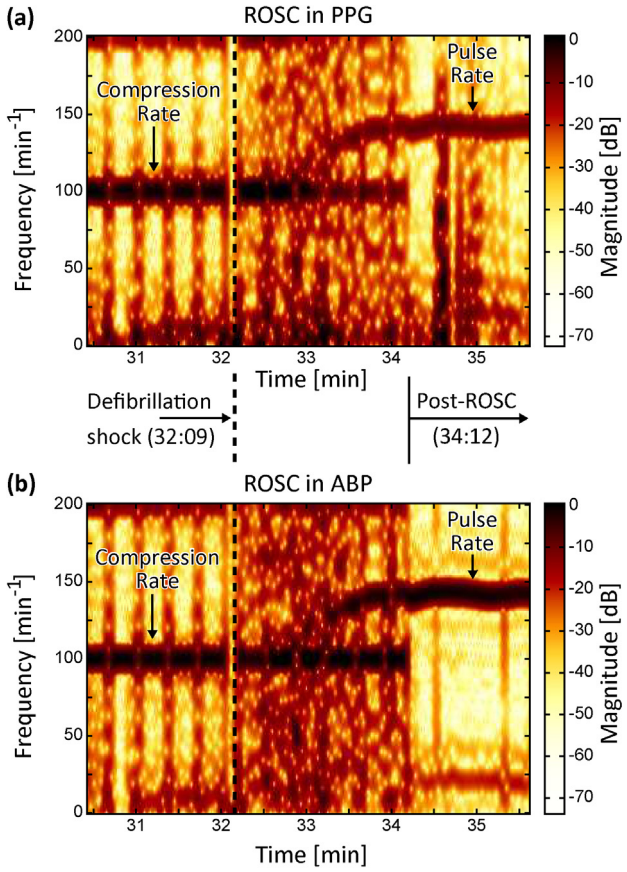

Fig. 3. Spectrograms of the PPG and ABP signals in a peri-arrest period. The defibrillation shock was applied at 32:09 (dashed line). Chest compressions were stopped at 34:12. (a) Spectrogram of the PPG signal. At 34:30 the ventilation bag is uncoupled and the ventilator is attached, which results in a broad spectral motion artifact. (b) Spectrogram of the ABP signal. The spectrograms were obtained by partitioning the 0.1-Hz high-pass filtered signals in segments of 10 s with 90% overlap and applying a Hamming window. For convenient time referencing, the time axis corresponds to the center of each segment. The spectrograms have been normalized by the magnitude of the spectral compression component in the signal at the beginning of the trace shown. This is the same animal (#R1) as in Figs. 2 and 4d. ABP: arterial blood pressure; PPG: photoplethysmography; ROSC: return of spontaneous circulation.

about 125 min^{-1}, increasing to about 140 min^{-1}, and continuing when compressions were stopped. In this controlled setting, this component could only be a spontaneous pulse.

For all 12 animals, the PPG and ABP frequency spectra showed strong resemblance (Fig. 4). For animals without return of spontaneous pulse, the spectra only contained components due to the automated chest compressions (Fig. 4a–c). For animals with ROSC, the spontaneous pulse resulted in one or more additional components in the spectra (Fig. 4d–l). The pulse rate could be readily identified in the frequency spectra in eight out of nine cases. In Fig. 4f, the pulse rate was close to the compression rate and was only observable as a small broadening in the right flanks of the chest compression components.

3.3. Trend of relative PPG amplitude

In a case of transient ROSC (Fig. 5), CPR was stopped when ROSC was diagnosed, and restarted when the circulation was considered inadequate. During the period without compressions, the spectrograms of the PPG and ABP signals (Fig. 5a and b) showed a spontaneous pulse. The pulse amplitude in the PPG time trace decreased in this period and had almost disappeared when compressions were restarted (Fig. 5c).

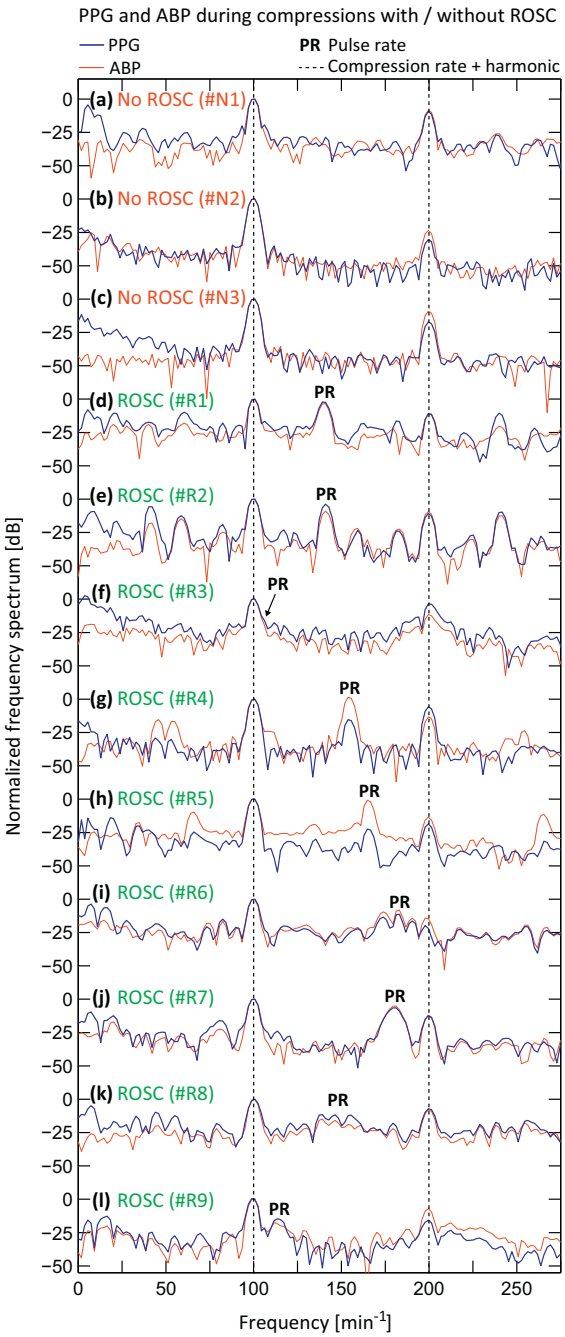

Fig. 4. Pulse rate behavior during CPR in the PPG and ABP spectra of various animals. Dashed lines indicate the automated chest compression frequency at 100 min^{-1} and its harmonic at 200 min^{-1}. (a)–(c) Animals without ROSC. (d)–(l) Animals with ROSC. The pulse rate has been determined by visually inspecting the corresponding spectrograms. Spectra (a)–(l) have been determined from a segment of 20 s containing the last series of 30 chest compressions in each experiment. A 0.1-Hz high-pass filter and a Hamming window were applied before determining the spectra via Fourier transformation. Each spectrum has been normalized by the magnitude of the spectral compression component in the signal. ABP: arterial blood pressure; CPR: cardiopulmonary resuscitation; PPG: photoplethysmography; PR: pulse rate; ROSC: return of spontaneous circulation.

4. Discussion

The aim of the present study was to investigate whether PPG signals can be used to detect the presence or absence of spontaneous cardiac-induced pulsations during CPR. This could be a first step toward objectifying and shortening ROSC determination. Raw PPG data acquired with a custom-built photoplethysmograph were

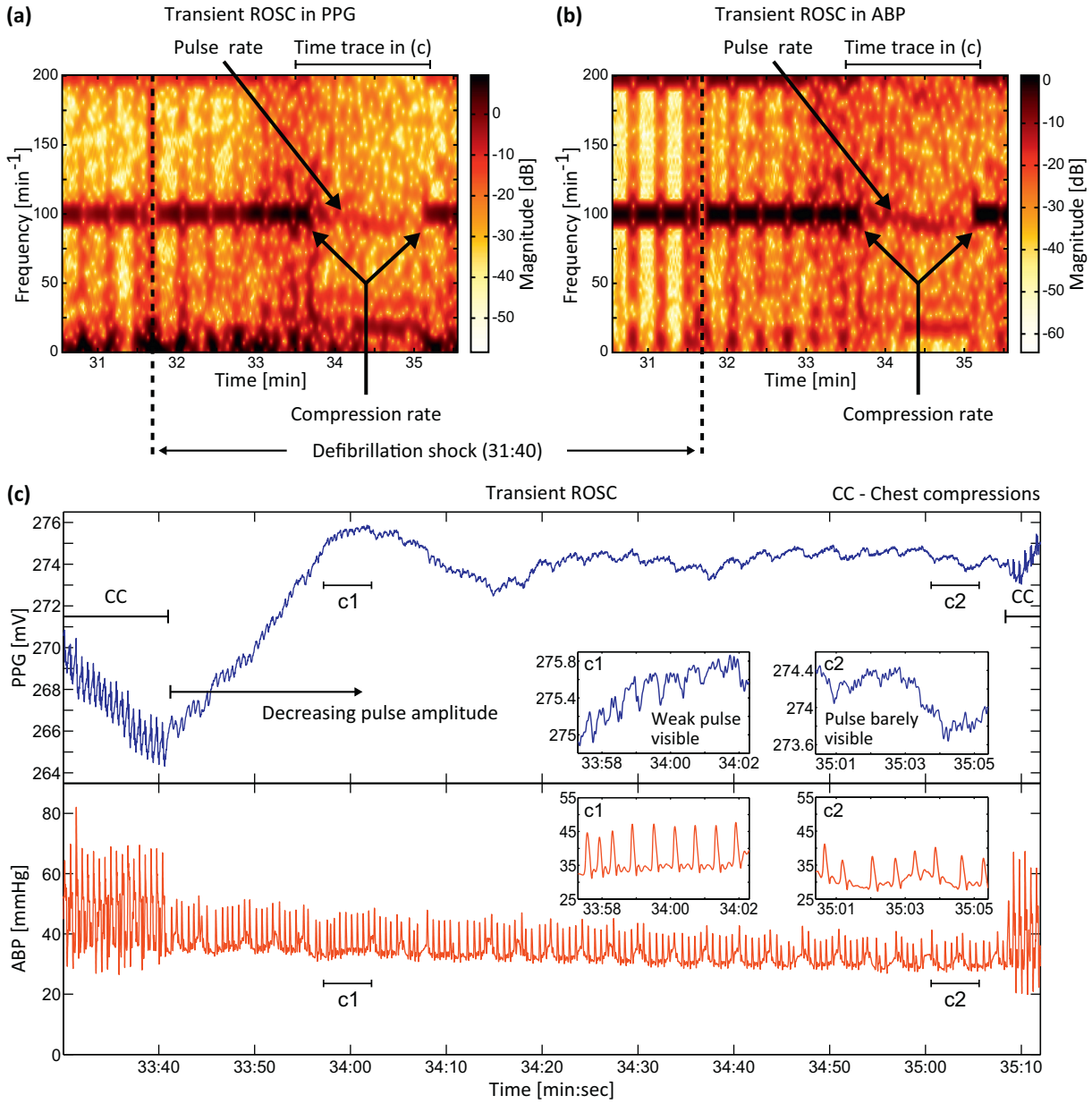

Fig. 5. Decreasing pulse amplitude observable in PPG signal during transient ROSC. The defibrillation shock was applied at 31:40 (dashed line). CPR was stopped at 33:41, and restarted at 35:08. (a) Spectrogram of the PPG signal. (b) Spectrogram of the ABP signal. (c) Time traces of the PPG and ABP signals. The insets show two close-ups of the PPG and ABP waveforms. The spectrograms were obtained by partitioning the 0.1-Hz high-pass filtered signals in segments of 10 s with 90% overlap and applying a Hamming window. For convenient time referencing, the time axis corresponds to the center of each segment. The spectrograms have been normalized by the magnitude of the spectral compression component in the signal at the beginning of the trace shown. This is the same animal (#N1) as in Fig. 4a. ABP: arterial blood pressure; CC: chest compressions; PPG: photoplethysmography; ROSC: return of spontaneous circulation.

analyzed retrospectively in both time and frequency domains, using the ABP as a reference.

Although PPG and ABP waveforms have comparable morphology, it is important to note that ABP represents the blood pressure in the macrovasculature, while PPG reflects the blood volume pulse in the microvasculature.[26,28] As such, besides ABP, also arteriolar vasomotor tone and microvascular shunting affect the PPG waveform.[26–28] Therefore, during CPR, decreased ABP and increased vasomotor tone might significantly reduce the pulsatility in the PPG waveform while ABP pulsatility remains. Nevertheless, the data show that presence and rate of a spontaneous cardiac pulse could be determined from a PPG signal during CPR. A PPG time trace could be used to detect spontaneous pulses during ventilation pauses, as illustrated in Fig. 2c. However, Fig. 2c also illustrates that it can be challenging to directly identify the spontaneous pulses in the PPG time trace during compressions. To resolve this, a spectral analysis was performed, which facilitates the identification of a spontaneous pulse and its rate during chest compressions, as shown in Figs. 3 and 4d, e, g–l.

During CPR, a PPG measurement performed at a stable site has the advantage of being less sensitive to motion artifacts than a TTI measurement, which is performed at the chest. Furthermore, PPG shows pulse presence faster than NIRS. However, the frequency spectra also show that real-time identification of a spontaneous cardiac pulse in the PPG signal during automated CPR may not be straightforward in all cases. Three complicating situations can occur, the first two being specifically related to ongoing chest compressions. First, the presence of spectral components in addition to the pulse and compression rates (and their harmonics) can complicate the identification of the spontaneous pulse component

(Fig. 4d,e, and h–l). As these additional spectral components seem to arise at rates equal to the sum and difference of the compression and pulse rates, they may indicate an interaction between the chest compressions and the spontaneous cardiac activity. Second, when the pulse rate is close to the compression rate, the spontaneous pulse is difficult to identify in the spectrum (Figs. 4f, 5a, and 5b). And third, in general it can be technically challenging to identify a rapidly varying pulse rate in the spectrum, because variations in the rate result in a less well-defined, broadened peak in the spectrum (Fig. 4i and k). Furthermore, in case of manual CPR where the compression rate may fluctuate, an independent measurement of the manual compression rate[2,4,5] can potentially be used to identify the chest compression rate in the spectrum and distinguish it from a spontaneous pulse rate.

In addition to using PPG signals to obtain feedback on manual chest compression rates as described by Xu et al[29] and Spittal,[31] our data show that PPG signals can offer information about the presence or absence of a spontaneous cardiac pulse during CPR, making it potentially useful to support ROSC detection. Via PPG-based screening for pulse during ongoing compressions, absence of spontaneous cardiac activity can be noted which may prevent unnecessary or lengthy pauses in chest compressions for examination of ROSC. Furthermore, detection of return of spontaneous pulse during ongoing compressions may guide administration of vasopressors, as vasopressors may have detrimental effects when administered following a shock that has resulted in a perfusing rhythm.[1,2] The broad spectral activity in the PPG during CPR following the defibrillation shock (Figs. 3 and 5) may provide an early indication of start-up of spontaneous cardiac output, or other muscular activity. Reinstitution of CPR may be guided by fading of a spontaneous pulse in the PPG, which may indicate loss of a perfusing rhythm (Fig. 5c). These observations warrant further research on the potential of PPG as a ROSC indicator.

This study, however, has some limitations. First, an animal model is never fully representative of clinical scenarios, but it allowed comparison between PPG signals and invasively measured ABP in a controlled environment. Second, suturing the PPG sensor to the nose to limit excessive motion artifacts is not representative of good clinical practice. However, the goal of this study was determining the feasibility of identifying a spontaneous pulse in a PPG signal during CPR, and not dealing with the technical solution for corrupting motion. Finally, to be able to detect a spontaneous pulse in humans during CPR in clinical practice, a central-site PPG measurement (e.g., from the facial region) may be preferred over a peripheral site, as centralization and the associated vasoconstriction can severely compromise peripheral pulsatile blood flow.[2,36,37]

5. Conclusions

After ROSC, cardiac pulses could be observed in the nasal PPG waveform during ventilation pauses. During chest compressions the contribution of spontaneous cardiac activity could be identified by analyzing the PPG frequency spectrum, when the pulse and compression rates were sufficiently distinct. We conclude that PPG has potential to support detection of ROSC during CPR.

Conflicts of interest

None of the authors have monetary or other interests which may have influenced this paper. Ralph Wijshoff was supported by a grant from NL Agency, IOP Photonic Devices, IPD083359 HIP – Hemodynamics by Interferometric Photonics. Gerrit J. Noordergraaf is a consultant for Philips Research.

Acknowledgements

This work was supported by NL Agency, IOP Photonic Devices, IPD083359 HIP – Hemodynamics by Interferometric Photonics. The authors like to thank Mr. Alex Hanssen, Ms. Wilma Janssen-Kessel, and Mr. Maikel School of the Central Animal Laboratory of the Radboud University Nijmegen Medical Center, and Dr. Matthijs Kox, Ms. Francien van de Pol, and Ms. Kim Timmermans from the Radboud University Nijmegen Medical Center for their assistance during the preparation and conduction of the experiments. The authors are grateful to Mr. Ben Wassink of VDL ETG Research bv for technical assistance.

References

1. Deakin CD, Nolan JP, Soar J, et al. European Resuscitation Council guidelines for resuscitation 2010 Section 4. Adult advanced life support. Resuscitation 2010;81:1305–52.
2. Neumar RW, Otto CW, Link MS, et al. Part 8: adult advanced cardiovascular life support: 2010 American Heart Association guidelines for cardiopulmonary resuscitation and emergency cardiovascular care. Circulation 2010;122:S729–67.
3. Berg RA, Sanders AB, Kern KB, et al. Adverse hemodynamic effects of interrupting chest compressions for rescue breathing during cardiopulmonary resuscitation for ventricular fibrillation cardiac arrest. Circulation 2001;104:2465–70.
4. Wik L, Kramer-Johansen J, Myklebust H, et al. Quality of cardiopulmonary resuscitation during out-of-hospital cardiac arrest. JAMA 2005;293:299–304.
5. Christenson J, Andrusiek D, Everson-Stewart S, et al. Chest compression fraction determines survival in patients with out-of-hospital ventricular fibrillation. Circulation 2009;120:1241–7.
6. Eberle B, Dick WF, Schneider T, Wisser G, Doetsch S, Tzanova I. Checking the carotid pulse check: diagnostic accuracy of first responders in patients with and without a pulse. Resuscitation 1996;33:107–16.
7. Ochoa FJ, Ramalle-Gómara E, Carpintero JM, García A, Saralegui I. Competence of health professionals to check the carotid pulse. Resuscitation 1998;37:173–5.
8. Moule P. Checking the carotid pulse: diagnostic accuracy in students of the healthcare professions. Resuscitation 2000;44:195–201.
9. Tibballs J, Russell P. Reliability of pulse palpation by healthcare personnel to diagnose paediatric cardiac arrest. Resuscitation 2009;80:61–4.
10. Grmec Š, Križmarič M, Mally Š, Koželj A, Špindler M, Lešnik B. Utstein style analysis of out-of-hospital cardiac arrest—Bystander CPR and end expired carbon dioxide. Resuscitation 2007;72:404–14.
11. Pokorná M, Nečas E, Kratochvíl J, Skřipský R, Andrlík M, Franěk O. A sudden increase in partial pressure end-tidal carbon dioxide ($P_{ET}CO_2$) at the moment of return of spontaneous circulation. J Emerg Med 2010;38:614–21.
12. Heradstveit BE, Sunde K, Sunde G-A, Wentzel-Larsen T, Heltne J-K. Factors complicating interpretation of capnography during advanced life support in cardiac arrest—A clinical retrospective study in 575 patients. Resuscitation 2012;83:813–8.
13. Davis DP, Sell RE, Wilkes N, et al. Electrical and mechanical recovery of cardiac function following out-of-hospital cardiac arrest. Resuscitation 2013;84:25–30.
14. Paradis NA, Martin GB, Rivers EP, et al. Coronary perfusion pressure and the return of spontaneous circulation in human cardiopulmonary resuscitation. JAMA 1990;263:1106–13.
15. Rivers EP, Lozon J, Enriquez E, et al. Simultaneous radial, femoral, and aortic arterial pressures during human cardiopulmonary resuscitation. Crit Care Med 1993;21:878–83.
16. Rivers EP, Martin GB, Smithline H, et al. The clinical implications of continuous central venous oxygen saturation during human CPR. Ann Emerg Med 1992;21:1094–101.
17. Losert H, Risdal M, Sterz F, et al. Thoracic-impedance changes measured via defibrillator pads can monitor signs of circulation. Resuscitation 2007;73:221–8.
18. Risdal M, Aase SO, Kramer-Johansen J, Eftestøl T. Automatic identification of return of spontaneous circulation during cardiopulmonary resuscitation. IEEE Trans Biomed Eng 2008;55:60–8.
19. Stecher FS, Olsen J-A, Stickney RE, Wik L. Transthoracic impedance used to evaluate performance of cardiopulmonary resuscitation during out of hospital cardiac arrest. Resuscitation 2008;79:432–7.
20. Reynolds JC, Salcido D, Koller AC, et al. Tissue oximetry by near-infrared spectroscopy in a porcine model of out-of-hospital cardiac arrest and resuscitation. Resuscitation 2013;84:843–7.
21. Kämäräinen A, Sainio M, Olkkola KT, Huhtala H, Tenhunen J, Hoppu S. Quality controlled manual chest compressions and cerebral oxygenation during in-hospital cardiac arrest. Resuscitation 2012;83:138–42.
22. Parnia S, Nasir A, Shah C, Patel R, Mani A, Richman P. A feasibility study evaluating the role of cerebral oximetry in predicting return of spontaneous circulation in cardiac arrest. Resuscitation 2012;83:982–5.
23. Ahn A, Nolan J, Parnia S. Cerebral oximetry in cerebral resuscitation after cardiac arrest. In: Vincent JL, editor. Annual update in intensive care and emergency medicine. Berlin, Heidelberg: Springer; 2013. p. 337–45.

24. Nagdyman N, Fleck TPK, Ewert P, Abdul-Khaliq H, Redlin M, Lange PE. Cerebral oxygenation measured by near-infrared spectroscopy during circulatory arrest and cardiopulmonary resuscitation. Br J Anaesth 2003;91:438–42.
25. Webster JG, editor. Design of pulse oximeters. New York: Taylor & Francis Group; 1997.
26. Allen J. Photoplethysmography and its application in clinical physiological measurement. Physiol Meas 2007;28:R1–39.
27. Shelley KH. Photoplethysmography: beyond the calculation of arterial oxygen saturation and heart rate. Anesth Analg 2007;105:S31–6.
28. Reisner A, Shaltis PA, McCombie D, Asada H. Utility of the photoplethysmogram in circulatory monitoring. Anesthesiology 2008;108:950–8.
29. Xu J, Zhu H, Wang Z, Yu X, Walline J. Why do not we use finger pulse oximeter plethysmograph waveform to monitor the effectiveness of cardiopulmonary resuscitation? Resuscitation 2011;82:959.
30. Moorthy SS, Dierdorf SF, Schmidt SI. Erroneous pulse oximeter data during CPR. Anesth Analg 1990;70:334–41.
31. Spittal MJ. Evaluation of pulse oximetry during cardiopulmonary resuscitation. Anaesthesia 1993;48:701–3.
32. Idris AH, Becker LB, Ornato JP, et al. Utstein-style guidelines for uniform reporting of laboratory CPR research. Circulation 1996;94:2324–36.
33. Steen S, Liao Q, Pierre L, Paskevicius A, Sjöberg T. Evaluation of LUCAS, a new device for automatic mechanical compression and active decompression resuscitation. Resuscitation 2002;55:285–99.
34. Kleinman ME, Chameides L, Schexnayder SM, et al. Part 14: Pediatric advanced life support: 2010 American Heart Association guidelines for cardiopulmonary resuscitation and emergency cardiovascular care. Circulation 2010;122:S876–908.
35. Hayes MJ, Smith PR. A new method for pulse oximetry possessing inherent insensitivity to artifact. IEEE Trans Biomed Eng 2001;48:452–61.
36. Branson RD, Mannheimer PD. Forehead oximetry in critically ill patients: the case for a new monitoring site. Respir Care Clin N Am 2004;10:359–67.
37. Pälve H. Reflection and transmission pulse oximetry during compromised peripheral perfusion. J Clin Monit Comput 1992;8:12–5.